

Luminescence of Eu^{3+} in $\text{GaN}(\text{Mg}, \text{Eu})$: Transitions from the ${}^5\text{D}_1$ level

A. K. Singh,^{1,2} K. P. O'Donnell,^{1,a)} P. R. Edwards,¹ D. Cameron,¹ K. Lorenz,³ M. J. Kappers,⁴ M. Boćkowski,⁵ M. Yamaga,⁶ and R. Prakash²

¹*SUPA Department of Physics, University of Strathclyde, 107 Rottenrow, Glasgow G4 0NG, Scotland, United Kingdom*

²*School of Materials Science and Technology, Indian Institute of Technology (BHU) Varanasi, Varanasi 221005, India*

³*IPFN, Instituto Superior Técnico, Universidade de Lisboa, Campus Tecnológico e Nuclear, Estrada Nacional 10, 2695-066 Bobadela LRS, Portugal*

⁴*Department of Materials Science and Metallurgy, University of Cambridge, 27 Charles Babbage Road, Cambridge CB3 0FS, England, United Kingdom*

⁵*Institute of High Pressure Physics PAS, Sokolowska 29/37, 01-142 Warsaw, Poland*

⁶*Department of Mathematical and Design Engineering, Gifu University, Gifu 501-1193, Japan*

(Received 22 August 2017; accepted 30 November 2017; published online 14 December 2017)

Eu-doped $\text{GaN}(\text{Mg})$ exemplifies hysteretic photochromic switching between two configurations, Eu0 and $\text{Eu1}(\text{Mg})$, of the same photoluminescent defect. Using the above-bandgap excitation, we studied the temperature dependence of photoluminescence (TDPL) of transitions from the excited ${}^5\text{D}_1$ level of Eu^{3+} for both configurations of this defect. During sample cooling, ${}^5\text{D}_1 \rightarrow {}^7\text{F}_{0,1,2}$ transitions of Eu0 manifest themselves at temperatures below ~ 200 K, while those of $\text{Eu1}(\text{Mg})$ appear only during switching. The observed line positions verify crystal field energies of the ${}^7\text{F}_{0,1,2}$ levels. TDPL profiles of ${}^5\text{D}_1 \rightarrow {}^7\text{F}_1$ and ${}^5\text{D}_0 \rightarrow {}^7\text{F}_J$ transitions of Eu0 show an onset of observable emission from the ${}^5\text{D}_1$ level coincident with the previously observed, but hitherto unexplained, decrease in the intensity of its ${}^5\text{D}_0 \rightarrow {}^7\text{F}_J$ emission on cooling below 200 K. Hence, the ${}^5\text{D}_0 \rightarrow {}^7\text{F}_J$ TDPL anomaly signals a back-up of ${}^5\text{D}_1$ population due to a reduction in phonon-assisted relaxation between ${}^5\text{D}_1$ and ${}^5\text{D}_0$ levels at lower temperatures. We discuss this surprising result in the light of temperature-dependent transient luminescence measurements of Eu0 . © 2017 Author(s). All article content, except where otherwise noted, is licensed under a Creative Commons Attribution (CC BY) license (<http://creativecommons.org/licenses/by/4.0/>). <https://doi.org/10.1063/1.5001143>

Since the millennium, the doping of GaN with europium has gained considerable attention^{1–4} on the strength of its potential applications in the fabrication of red light emitting diodes,^{5–9} with particular emphasis on the strongest, “hypersensitive,” transitions of Eu^{3+} , denoted ${}^5\text{D}_0 \rightarrow {}^7\text{F}_2$, near 620 nm. In general, photoluminescence (PL) spectra of Eu-doped GaN feature emission from multiple “sites” suggest the possibility of modifying the local environment of Eu ions, thereby increasing the luminescence yield, by impurity or defect engineering.^{7,10,11} Utilising a variety of sample preparation techniques, a number of researchers recently reported that co-doping $\text{GaN}:\text{Eu}$ with magnesium, the commercially successful p-type dopant of III-nitride semiconductors, enhances Eu emission at room temperature and forms new defects.^{12–16}

One clear advantage of our favoured technique of preparing $\text{GaN}(\text{Mg}):\text{Eu}$ by high-temperature annealing of Eu-implanted p-type GaN , as opposed to *in situ* growth techniques, is that it leads to simpler spectra: the red emission at room temperature of annealed, implanted samples comes from a single centre, suggesting selective attraction between Eu and Mg atoms in the GaN lattice during annealing.¹⁶ This centre was found to show hysteretic photochromic switching (HPS) between two configurations of the same defect [labelled Eu0 and $\text{Eu1}(\text{Mg})$]; at low temperature, Eu0 spectral lines disappear and a spectrum of different symmetry,

corresponding to $\text{Eu1}(\text{Mg})$, replaces them: there is a *photochromic* transformation between alternate defect configurations, with the rate of switching dependent upon temperature, light intensity, and photon energy.^{17,18} The reverse process, switching $\text{Eu1}(\text{Mg})$ back to Eu0 , occurs when the sample warms above ~ 175 K; hence, the photochromism is *hysteretic* with temperature. In the simplest defect model, the $\text{Eu0}/\text{Eu1}(\text{Mg})$ defect comprises an Eu atom, substituting for Ga, in close association with Mg, also substitutional, bonded to a common N atom.¹⁷ We have ascribed the observed changes in the defect configuration to the well-known shallow-deep instability of the Mg-N bond length,¹⁹ in these experiments, the Eu spectrum *monitors* the disposition of the acceptor in the GaN lattice.¹⁸

The above-bandgap photo-excitation of GaN at 3.5 eV creates mobile electrons and holes and mimics their electrical injection in light emitting diodes; the excitation of emission from embedded Eu^{3+} ions therefore involves a cascade of decay processes. In both PL and EL, emission is dominated by transitions from the lowest excited ${}^5\text{D}$ state, namely, ${}^5\text{D}_0 \rightarrow {}^7\text{F}_J$ transitions, with the ${}^5\text{D}_0 \rightarrow {}^7\text{F}_2$ lines dominating by an order of magnitude. On the other hand, an approach to a complete spectroscopic analysis of the Eu-associated defects, such as that carried out for $\text{AlN}:\text{Eu}$ by Gruber *et al.*,²⁰ requires us to consider both transitions from ${}^5\text{D}_0$ to other states, such as ${}^7\text{F}_1$,¹⁷ and transitions from higher lying ${}^5\text{D}$ levels. For this reason, we have carried out a preliminary investigation of the ${}^5\text{D}_1 \rightarrow {}^7\text{F}_J$ emission of Eu^{3+} in

^{a)}E-mail: k.p.odonnell@strath.ac.uk

GaN(Mg). Following Favennec *et al.*,²¹ we use the temperature dependence of photoluminescence (TDPL) to gain further insights into the emission characteristics of the defects. The 5D_1 - 5D_0 energy separation is about 0.2 eV, equivalent to a temperature in excess of 2000 K. Assuming thermal equilibrium among 5D_J states, conventional spectroscopic wisdom would predict that emission involving 5D_1 levels should be very weak at room temperature, becoming even weaker at lower temperatures. In fact, the opposite is found to be the case.

Details of sample preparation and characterization have been reported previously.¹⁷ GaN samples doped with Mg to concentrations of $\sim 1.1 \times 10^{19} \text{ cm}^{-3}$ were implanted with various fluences of Eu^+ ($4 \times 10^{13} \text{ cm}^{-2}$ @ 70 keV, $8.5 \times 10^{13} \text{ cm}^{-2}$ @ 150 keV, and $3 \times 10^{14} \text{ cm}^{-2}$ @ 380 keV) along the surface normal, resulting in a quasi-uniform Eu concentration of $\sim 5 \times 10^{19} \text{ at/cm}^3$ from 20 to 75 nm below the sample surface. One sample was annealed at 1673 K under 10.5 kbar of N_2 to remove implantation damage. Conventional photoluminescence (PL) spectroscopy yields Eu^{3+} spectra of samples mounted in a He cryorefrigerator in the temperature range from ~ 10 K to 300 K, using a tripled Nd:YAG 355 nm, 20 mW CW laser (Cobolt Zouk); residual second harmonic laser emission at 532.2 nm provides a useful wavelength reference in some spectral regions. Transient PL intensity was measured using a pulsed 355 nm, Nd:YAG laser with a repetition rate of 10 Hz (Innolas, Spotlight 600) and recorded, at several different temperatures, on the strongest line originating on the 5D_0 level of the $\text{Eu}0$ configuration at ~ 619 nm. Data were acquired using an oscilloscope (Hameg HM1507) equipped with SP107 software. The decay time was calculated by monoexponential fitting of decay data, and the risetime was estimated as described later. Our attempts to record transient emission from 5D_1 failed due to the strong yellow band background in that spectral region (shown later in Fig. 2).

Figure 1 summarises typical results of a cooling run, from 295 K to 13 K (hereafter written as [295, 13 K]), obtained by plotting against temperature the mean PL intensities of transitions that terminate on the 7F_1 level. Considering the ${}^5D_0 \rightarrow {}^7F_1$ emission of $\text{Eu}0$, we first observe a rapid increase in intensity with cooling, in [295, 200 K], followed by an anomalous decrease, hitherto unexplained, in the range

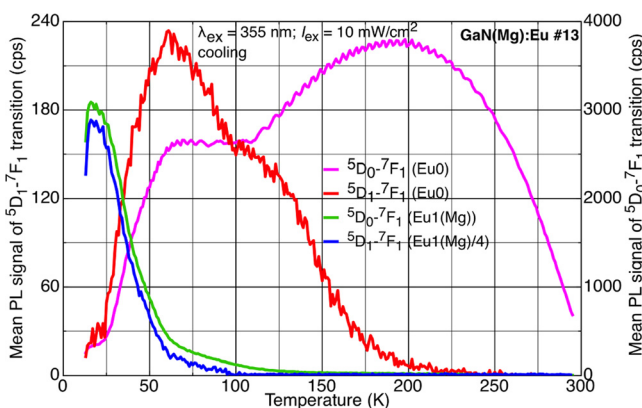


FIG. 1. Mean PL signal intensities of ${}^5D_1 \rightarrow {}^7F_1$ and ${}^5D_0 \rightarrow {}^7F_1$ transitions of Eu^{3+} for $\text{Eu}0$ and $\text{Eu}1(\text{Mg})$ configurations as a function of temperature recorded during cooling in the range [295, 13 K] under 355 nm excitation by a CW laser ($I_{\text{ex}} = 10 \text{ mW/cm}^2$).

[200, 120 K]. An intensity plateau in [120, 60 K] is succeeded by photochromic switching from $\text{Eu}0$ to $\text{Eu}1(\text{Mg})$ as the sample is further cooled towards the base temperature of the cryostat. Most of the switching occurs in a narrow range of temperature around 40 K, but a weak $\text{Eu}1(\text{Mg})$ signal appears at 150 K and grows slowly as the sample cools in the range [150, 70 K].

$\text{Eu}0$ transitions from the 5D_1 levels are also observed but only at temperatures below ~ 200 K. Figure 2 shows typical sample spectra at 100 K (featuring mainly $\text{Eu}0$ PL) and at 13 K [only $\text{Eu}1(\text{Mg})$]. The temperature-dependent PL profile of the ${}^5D_1 \rightarrow {}^7F_1$ transition of $\text{Eu}0$ (Fig. 1) shows an onset of emission below 200 K. In fact, a closer look at Fig. 1 reveals that the decrease in ${}^5D_0 \rightarrow {}^7F_1$ emission and the increase in ${}^5D_1 \rightarrow {}^7F_1$ emission intensities are complementary. Thus, the study of emission corresponding to ${}^5D_1 \rightarrow {}^7F_1$ transitions points the way to an explanation for the anomalous dependence of the ${}^5D_0 \rightarrow {}^7F_1$ PL of $\text{Eu}0$ in the temperature range [200, 120 K].

Figure 3 shows transient PL profiles, both in rise and in decay, for the $\text{Eu}0$ configuration, recorded by monitoring ${}^5D_0 \rightarrow {}^7F_2$ emission at 619 nm. The decay lifetime of 5D_0 increases with cooling but is nearly constant below 200 K. In addition, the 5D_0 level shows a risetime which increases markedly with decreasing temperature from less than about 10 μs at 275 K to $\sim 200 \mu\text{s}$ at 125 K, as estimated from the time taken for the signal to reach its peak.

The observation of ${}^5D_1 \rightarrow {}^7F_1$ transitions enables us to verify the crystal field splittings of the 7F_1 levels of Eu^{3+} ions and their energies.¹⁶ Table I summarises the line positions (wavelengths) and energy levels obtained by harmonising the

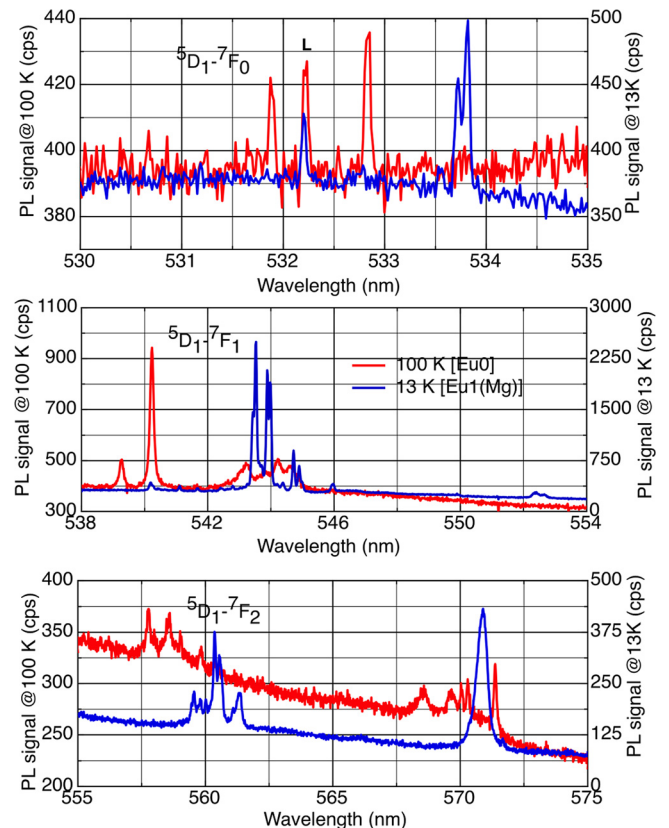


FIG. 2. PL spectra corresponding to ${}^5D_1 \rightarrow {}^7F_1$ transitions of Eu^{3+} ions recorded at 100 K (in predominantly $\text{Eu}0$ configuration) and at 13 K after switching [$\text{Eu}1(\text{Mg})$ configuration] (see text.).

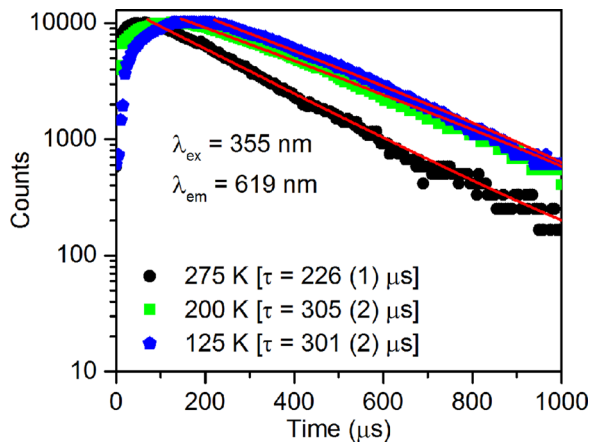


FIG. 3. PL rise and decay profiles of the 5D_0 level monitored at the strongest ${}^5D_0 \rightarrow {}^7F_2$ transition of Eu0 near 619 nm.

assignments of line positions to transitions arising on 5D_0 and 5D_1 levels, for each configuration. (The PL spectrum corresponding to ${}^5D_0 \rightarrow {}^7F_J$ transitions can be found in Ref. 17.) The PL spectrum was examined in high resolution; in regions of overlap, multiple Gaussian peak fitting helped us to determine accurate line positions. The energy positions of various levels and their crystal field splitting were calculated by using the ground state of Eu^{3+} (7F_0) as a reference. The PL spectrum corresponding to ${}^5D_1 \rightarrow {}^7F_0$ transitions of Eu0 recorded at 100 K shows emission peaks at 531.9 and 532.8 nm, corresponding to transition energies (energy positions of the 5D_1 level) of 18801 cm^{-1} and 18768 cm^{-1} . (The feature marked “L” at 532.2 nm is the laser second harmonic.) After Eu0 to Eu1(Mg) switching, the emission spectrum, recorded at 13 K, clearly shows three peaks at 533.5, 533.7, and 533.8 nm. These emission peaks correspond to crystal field splitting of the 5D_1 level into $|0\rangle$ and sublevels which mix the $|\pm 1\rangle$ states, denoted in Table I as ${}^5D_1(0)$, ${}^5D_1(1b)$, and ${}^5D_1(1a)$. In the Eu0 configuration, we expect ${}^5D_1(0) \rightarrow {}^7F_0$ transitions to be weak and in fact detect only 2 lines. The overall energy splittings of the 5D_1 level in the Eu0 and Eu1(Mg) configurations are $\sim 33 \text{ cm}^{-1}$ ($\sim 4.0 \text{ meV}$) and $\sim 10 \text{ cm}^{-1}$ (1.2 meV),

respectively. The difference in energy splitting of the 5D_1 levels of Eu0 and Eu1(Mg) therefore mirrors that found previously for their 7F_1 levels.¹⁷ These findings confirm that the crystal field acting on Eu1(Mg) is much more axial than that acting on Eu0: in other words, the Eu0 configuration is much less symmetric.

The relative intensities of Eu0 and Eu1(Mg) transitions also reflect their difference in symmetry in line with Judd-Ofelt theory.²² In some way similar to the strongest “hypersensitive” ${}^5D_0 \rightarrow {}^7F_2$ transition, ${}^5D_1 \rightarrow {}^7F_1$ is the most intense electric-dipole transition originating on the 5D_1 level. In the Eu0 configuration, the strongest ${}^5D_1 \rightarrow {}^7F_1$ peak observed at 540.2 nm (18512 cm^{-1}) corresponds to a transition from the lowest sublevel of 5D_1 to the lowest sublevel of 7F_1 , indicating the presence of thermalisation *within* the 5D_1 multiplet. The ${}^5D_1 \rightarrow {}^7F_1$ emission of the Eu1(Mg) configuration is strong and well resolved; each peak in this region shows a doublet character, related to very closely spaced ${}^5D_1(1b)$ and ${}^5D_1(1a)$ sublevels (18736 and 18733 cm^{-1}). The rather weak ${}^5D_1 \rightarrow {}^7F_2$ transitions contain emission peaks corresponding to transitions from multiple sublevels of 5D_1 to 7F_2 , as given in Table I. Noticeably, in the Eu1(Mg) configuration, the out-lying line corresponding to the ${}^5D_1 \rightarrow {}^7F_2$ transition is a singlet, similar to the situation for the ${}^5D_0 \rightarrow {}^7F_2$ transition, whereas the Eu0 configuration shows multiple peaks in the same region. This provides further information on the change in local symmetry around Eu^{3+} upon switching from Eu0 to Eu1(Mg) which requires further investigation with the aid of a complete crystal field analysis of the spectrum.

The TDPL intensity profile of ${}^5D_1 \rightarrow {}^7F_1$ transitions of Eu0 recorded during cooling (Fig. 1) reveals an onset of emission from 5D_1 at 200 K. Above 200 K, the 5D_1 level can relax quickly through multi-phonon emission to 5D_0 levels of Eu^{3+} , resulting in strong ${}^5D_0 \rightarrow {}^7F_J$ emission. The cooling of samples below 200 K inhibits non-radiative relaxation between 5D_1 and 5D_0 levels and causes a non-equilibrium back-up of population in the 5D_1 level, which results in the observed ${}^5D_1 \rightarrow {}^7F_J$ emission. This is further supported by the transient PL measurements. The 5D_0 lifetime increases from

TABLE I. Position of various energy levels/sublevels and emission wavelengths corresponding to ${}^5D_0 \rightarrow {}^7F_J$ and ${}^5D_1 \rightarrow {}^7F_J$ transitions of Eu^{3+} ions in Eu0 at 100 K and Eu1(Mg) at 13 K.

Eu0 ($\pm 3 \text{ cm}^{-1}$)				Eu1(Mg) ($\pm 3 \text{ cm}^{-1}$)			
${}^5D_1(0) = ?$, ${}^5D_1(1b) = 18802$, ${}^5D_1(1a) = 18768 \text{ cm}^{-1}$; ${}^5D_0 = 17038 \text{ cm}^{-1}$;				${}^5D_1(0) = 18743 \text{ cm}^{-1}$, ${}^5D_1(1b) = 18736 \text{ cm}^{-1}$, ${}^5D_1(1a) = 18733 \text{ cm}^{-1}$;			
${}^7F_2(0) = 1253 \text{ cm}^{-1}$, ${}^7F_2(1b) = 1200 \text{ cm}^{-1}$, ${}^7F_2(1a) = 906 \text{ cm}^{-1}$;				${}^5D_0 = 16980 \text{ cm}^{-1}$, ${}^7F_2(0) = 1204 \text{ cm}^{-1}$, ${}^7F_2(1b) = 923 \text{ cm}^{-1}$;			
${}^7F_2(2b) = 895 \text{ cm}^{-1}$, ${}^7F_2(2a) = 880 \text{ cm}^{-1}$, ${}^7F_1(0) = 439 \text{ cm}^{-1}$;				${}^7F_2(1a) = 898 \text{ cm}^{-1}$, ${}^7F_2(2b) = 877 \text{ cm}^{-1}$, ${}^7F_2(2a) = 874 \text{ cm}^{-1}$			
${}^7F_1(1b) = 393 \text{ cm}^{-1}$, ${}^7F_1(1a) = 258 \text{ cm}^{-1}$; ${}^7F_0 = 0 \text{ cm}^{-1}$				${}^7F_1(0) = 383 \text{ cm}^{-1}$, ${}^7F_1(1b) = 350 \text{ cm}^{-1}$, ${}^7F_1(1a) = 335 \text{ cm}^{-1}$; ${}^7F_0(0) = 0 \text{ cm}^{-1}$			
${}^5D_1 \rightarrow {}^7F_J$ transitions	Emission wavelength (nm)	${}^5D_0 \rightarrow {}^7F_J$ transitions	Emission wavelength (nm)	${}^5D_1 \rightarrow {}^7F_J$ transitions	Emission wavelength (nm)	${}^5D_0 \rightarrow {}^7F_J$ transitions	Emission wavelength (nm)
${}^5D_1 \rightarrow {}^7F_0$	531.9, 532.8	${}^5D_0 \rightarrow {}^7F_0$	586.9	${}^5D_1 \rightarrow {}^7F_0$	533.5, 533.7, 533.8	${}^5D_0 \rightarrow {}^7F_0$	588.9
${}^5D_1 \rightarrow {}^7F_1$	539.3, 540.2	${}^5D_0 \rightarrow {}^7F_1$	595.9	${}^5D_1 \rightarrow {}^7F_1$	543.4, 543.5	${}^5D_0 \rightarrow {}^7F_1$	600.8
	543.3, 543.9		600.8		543.9, 544		601.3
	544.7, 544.9		602.7		544.3, 545.2		602.7
	557.7, 558.6		618.9		559.5, 559.6		620.6
${}^5D_1 \rightarrow {}^7F_2$	559.9	${}^5D_0 \rightarrow {}^7F_2$	619.5	${}^5D_1 \rightarrow {}^7F_2$	559.8, 560.0	${}^5D_0 \rightarrow {}^7F_2$	620.9
	560.5		619.9		560.4, 560.5		621.8
	568.6, 569.6		631.4		561.2, 561.3		622.7
	570.3, 571.3		633.5		570.9		633.9

275 K to 200 K and becomes constant at lower temperatures; the risetime increases sharply with decreasing temperature. In a GaN:Eu sample, Bodiou *et al.*²³ measured a short 5D_1 lifetime and proposed that the risetime of the 5D_0 level indicates “an intermediate step through the 5D_1 level”.

Put simply, emission from 5D_1 occurs when the risetime of emission from 5D_0 exceeds the lifetime of the 5D_1 transitions. This condition is met at temperatures lower than ~ 200 K. While the effects of thermalisation *within* the excited state manifold of 5D_1 is evident in the spectral intensities, thermalisation does not apply between levels at low temperature, as pointed out by Binnemans,²⁴ since the relative population of these states is determined mainly by details of the excitation cascade, filling different states at different rates. At higher temperatures, Eu^{3+} ions can relax into the 5D_0 level through the interaction with the high-energy phonons of GaN. A relatively fast non-radiative interaction between the two levels at higher temperatures leads to a correlated increase in emission from 5D_0 at the expense of 5D_1 .

In summary, the detailed investigation of $^5D_1 \rightarrow ^7F_J$ and $^5D_0 \rightarrow ^7F_J$ line positions enables us to confirm the Eu^{3+} 7F_J level energies and their crystal field splittings, in both Eu0 and Eu1(Mg) configurations of the same defect. $^5D_1 \rightarrow ^7F_1$ is the most intense (hypersensitive) electric-dipole transition originating on the 5D_1 level in GaN(Mg):Eu samples. A comparative temperature-dependent study of PL intensity of the $^5D_1 \rightarrow ^7F_1$ and $^5D_0 \rightarrow ^7F_1$ transitions and of the PL decay of the strongest $^5D_1 \rightarrow ^7F_1$ and $^5D_0 \rightarrow ^7F_2$ transitions provides an explanation for the anomalous decrease in Eu0 emission intensity of $^5D_0 \rightarrow ^7F_J$ transitions during [200, 120 K] cooling. Thus, the results presented in this paper fully explain the TDPL profile of $^5D_0 \rightarrow ^7F_J$ transitions during cooling and also provide information regarding the temperature-dependent transient behaviour of the 5D_0 level in the Eu0 configuration.

K.P.O'D., P.R.E. and A.K.S. acknowledge funding from EPSRC, UK (EP/N00275X/1). The authors thank Professor S. B. Rai, BHU, for access to his laboratory for lifetime measurements. The data presented in this paper are available for download from <https://doi.org/10.15129/43f1e86a-33f5-4e25-8077-ef211c91666d>.

- ¹J. Heikenfeld, M. Garter, D. S. Lee, R. Birkhahn, and A. J. Steckl, *Appl. Phys. Lett.* **75**, 1189 (1999).
- ²K. Wang, R. W. Martin, K. P. O'Donnell, V. Katchkanov, E. Nogales, K. Lorenz, E. Alves, S. Ruffenach, and O. Briot, *Appl. Phys. Lett.* **87**, 112107 (2005).
- ³B. Mitchell, D. Lee, D. Lee, A. Koizumi, J. Poplawsky, Y. Fujiwara, and V. Dierolf, *Phys. Rev. B* **88**, 121202(R) (2013).
- ⁴H. Sekiguchi, M. Sakai, T. Kamada, H. Tateishi, A. Syouji, and A. Wakahara, *Appl. Phys. Lett.* **109**, 151106 (2016).
- ⁵A. J. Steckl, J. Heikenfeld, D. S. Lee, and M. Garter, *Mater. Sci. Eng. B* **81**, 97 (2001).
- ⁶R. Mueller-Mach, G. O. Mueller, M. R. Krames, and T. Trotter, *IEEE J. Sel. Top. Quantum Electron.* **8**, 339 (2002).
- ⁷K. P. O'Donnell and B. Hourahine, *Eur. Phys. J. Appl. Phys.* **36**, 91 (2006).
- ⁸A. Wakahara, H. Sekiguchi, H. Okada, and Y. Takagi, *J. Lumin.* **132**, 3113 (2012).
- ⁹M. Ishii, A. Koizumi, and Y. Fujiwara, *Appl. Phys. Lett.* **107**, 082106 (2015).
- ¹⁰I. S. Roqan, K. P. O'Donnell, R. W. Martin, P. R. Edwards, S. F. Song, A. Vantomme, K. Lorenz, E. Alves, and M. Boćkowski, *Phys. Rev. B* **81**, 085209 (2010).
- ¹¹Z. Fleischman, C. Munasinghe, A. J. Steckl, A. Wakahara, J. Zavada, and V. Dierolf, *Appl. Phys. B* **97**, 607 (2009).
- ¹²D. Lee, A. Nishikawa, Y. Terai, and Y. Fujiwara, *Appl. Phys. Lett.* **100**, 171904 (2012).
- ¹³H. Sekiguchi, Y. Takagi, T. Otani, H. Okada, and A. Wakahara, *J. Appl. Phys.* **113**, 013105 (2013).
- ¹⁴J. K. Mishra, T. Langer, U. Rossow, S. Shvarkov, A. Wieck, and A. Hangleiter, *Appl. Phys. Lett.* **102**, 061115 (2013).
- ¹⁵B. Mitchell, D. Lee, D. Lee, Y. Fujiwara, and V. Dierolf, *Appl. Phys. Lett.* **103**, 242105 (2013).
- ¹⁶K. P. O'Donnell, P. R. Edwards, M. J. Kappers, K. Lorenz, E. Alves, and M. Boćkowski, *Phys. Status Solidi C* **11**, 662 (2014).
- ¹⁷K. P. O'Donnell, P. R. Edwards, M. Yamaga, K. Lorenz, M. J. Kappers, and M. Boćkowski, *Appl. Phys. Lett.* **108**, 022102 (2016).
- ¹⁸A. K. Singh, K. P. O'Donnell, P. R. Edwards, K. Lorenz, M. J. Kappers, and M. Boćkowski, *Sci. Rep.* **7**, 41982 (2017).
- ¹⁹S. Lany and A. Zunger, *Appl. Phys. Lett.* **96**, 142114 (2010); J. L. Lyons, A. Janotti, and C. G. Van de Walle, *Phys. Rev. Lett.* **108**, 156403 (2012); J. J. Davies, *Phys. Rev. B* **87**, 235208 (2013).
- ²⁰J. B. Gruber, U. Vetter, T. Taniguchi, G. W. Burdick, H. Hofsass, S. Chandra, and D. K. Sardar, *J. Appl. Phys.* **110**, 023104 (2011).
- ²¹P. N. Favenec, H. L'Haridon, M. Salvi, D. Moutonnet, and Y. Le Gillou, *Electron. Lett.* **25**, 718 (1989).
- ²²B. R. Judd, *Phys. Rev.* **127**, 750 (1962); G. S. Ofelt, *J. Chem. Phys.* **37**, 511 (1962).
- ²³L. Bodiou, A. Braud, J.-L. Doualan, R. Moncorgé, J. H. Park, C. Munasinghe, A. J. Steckl, K. Lorenz, E. Alves, and B. Daudin, *J. Appl. Phys.* **105**, 043104 (2009).
- ²⁴K. Binnemans, *Coord. Chem. Rev.* **295**, 1 (2015).